Accepted Manuscript

Electrochemical pathway for the quantification of SERS enhancement factor

Arumugam Sivanesan, Witold Adamkiewicz, Govindasamy Kalaivani, Agnieszka Kamińska, Jacek Waluk, Robert Hołyst, Emad L. Izake

Please cite this article as: Arumugam Sivanesan, Witold Adamkiewicz, Govindasamy Kalaivani, Agnieszka Kamińska, Jacek Waluk, Robert Hołyst, Emad L. Izake, Electrochemical pathway for the quantification of SERS enhancement factor, *Electrochemistry Communications* (2014), doi: 10.1016/j.elecom.2014.10.007

Electrochemical pathway for the quantification of SERS enhancement factor

Arumugam Sivanesan,[*ab] Witold Adamkiewicz,[a] Govindasamy Kalaivani,[b] Agnieszka

Kamińska,[*a] Jacek Waluk,[a] Robert Hołyst[a] and Emad L. Izake[b]

a Institute of Physical Chemistry, Polish Academy of Sciences, Kasprzaka 44/52, 01-224 Warsaw, Poland

b School of Chemistry, Physics and Mechanical Engineering, Queensland University of Technology, Brisbane, Queensland, Australia

* Corresponding authors

E-mail address: asnesan@gmail.com; sivanesan.arumugam@qut.edu.au (A. Sivanesan) Tel: +61 07 3138 0607

E-mail address: akamin@ichf.edu.pl (A. Kamińska) Tel: +48 22 343 32 28

Abstract

This communication presents a new pathway for the more precise quantification of surface-enhanced Raman scattering (SERS) enhancement factor via deducing resonance Raman scattering (RRS) effect from surface-enhanced resonance Raman scattering (SERRS). To achieve this, a self-assembled monolayer of 1,8,15,22-tetraaminophthalocyanatocobalt(II) (4α-Co^{II}TAPc) is formed on plasmon inactive glassy carbon (GC) and plasmon active GC/AuNPs surface. The surfaces are subsequently used as common probes for electrochemical and Raman (RRS and SERRS) studies. The most crucial parameters required for the quantification of SERS substrate enhancement factor (SSEF) such as real surface area of GC/AuNPs substarte and the number of 4α-Co^{II}TAPc molecules contributing to RRS (on GC) and SERRS (on GC/AuNPs) are precisely estimated by cyclic voltammetry experiments. The present approach of SSEF quantification can be applied to varieties of surfaces by choosing an appropriate laser line and probe molecule for each surface.

1. Introduction

Nowadays surface-enhanced Raman spectroscopy (SERS) is becoming a popular ultrasensitive analytical technique [1, 2]. Nevertheless, the most important issue regarding SERS is the precise quantification of substrate enhancement factor (SSEF) i.e., the magnitude of the enhancement. Although wide varieties of SERS substrates have been produced within the last four decades, there is still no standard procedure to accurately quantify the SSEF. This causes the SERS technique not to be fully recognized as an accurate analytical tool.

Traditionally, the average substrate enhancement factor is quantified by the following equation [3-5]:

$$\text{SSEF} = \frac{I_{\text{SERS}} \cdot N_{\text{Vol}}}{I_{\text{RS}} \cdot N_{\text{Surf}}} \qquad (1)$$

Where N_{Vol} is the average number of molecules in the scattering volume (V) for the Raman (non-SERS) measurement, and N_{Surf} is the average number of adsorbed molecules in the scattering volume of the SERS experiments.

However, in the above equation, N_{Vol} and N_{Surf} are estimated by some assumptions and approximations and not via entire experimental measurements. In addition, the equation does not address the Raman cross-section of the chromophore as it significantly varies between solution and on SERS substrate because of solvent effect, aggregation effect and charge-transfer effect.

Recently, Le Ru and coworkers attempted to address some of the issues by proposing modified version of equation 1 [6].

$$\text{SSEF} = \frac{I_{\text{SERS}} \cdot (c_{\text{RS}} H_{\text{eff}})}{I_{\text{RS}} \cdot (\mu_{\text{M}} \mu_{\text{S}} A_{\text{M}})} \qquad (2)$$

Here H_{eff} is the effective height of the scattering volume, μ_M is the surface density of the individual nanostructures producing the enhancement, μ_S is the surface density of the molecules on the surface, and A_M represents the surface area of the SERS substrate. Although the above equation is assumed to give more rigorous estimation of SSEF when compared to equation 1, it is still very difficult to experimentally estimate some of the involved parameters with precision. Further, precise estimation of Raman cross-section in both solution and on SERS substrate still hangs on in equation 2.

To solve most of the above issues, this communication present a simplified and renewed approach for the quantification of SSEF with improved precision. To achieve this, we combined electrochemistry together with Raman scattering and precisely determined the real surface area of the SERS substrate as well as the number of probe molecules contributed to Raman (RRS and SERRS) effect. Further, by carrying out both RRS and SERRS on solid surfaces, most of the major issues associated with Raman-cross section has been avoided.

2. Outline of Renewed Approach

Recently, we employed the equation given by Hildebrandt et.al [7] for the quantification of SSEF for silver colloids [7-10]. The modified form of that equation is:

$$\text{SSEF} = \frac{I_{\text{SERRS}} \cdot c_{\text{RRS}}}{I_{\text{RRS}} \cdot c_{\text{SERRS}}} \qquad (3)$$

Here, c_{RRS} and c_{SERRS} are the concentrations of molecules involved in RRS and SERRS, respectively. The parameter shielding constant (k) is removed from the original equation [7] since the SERRS experiments in the present work have been carried out on solid substrate with a monolayer of probe molecule.

4

The basic principle that underlines our approach for the average quantification of SSEF is to deduct RRS contribution from overall SERRS outcome. To achieve this, demonstrating both RRS and SERRS in solid surfaces modified with a monolayer of electro- and Raman-active probe molecule is crucial. By carrying out both RRS (plasmon inactive) and SERRS (plasmon active) on surfaces having a monolayer of electro- and Raman- active probe, one can avoid the quantification of parameters such as focal volume, solvent effect, shielding effect and inner filter effect. Further, the parameters c_{RRS}, and c_{SERRS} and real surface area of SERS substrate can be precisely estimated by electrochemical method. We elected the compound 1,8,15,22-tetraaminophthalocyanatocobalt(II) (4α-Co^{II}TAPc) as it satisfies the sought criteria for the chromophore in our experiments. It is a very good redox-active molecule with strong absorption band around 750 nm. Moreover, it forms a stable monomolecular film on GC, Au, Ag and indium tin oxide (ITO) [11-13].

In our approach is, we assumed that Raman cross-section remains similar on both surfaces. Actually, RRS effect is directly related to the Raman cross-section of the chromophore which is then depends on charge-transfer, solvent and aggregation effect [6]. Nevertheless, in the present experimental conditions, the Raman cross-section exclusively depends on charge-transfer effect i.e. the chemical enhancement factor (CHEF) since 4α-Co^{II}TAPc forms a monolayer on the GC and GC/Au substrates. It is well-known that the contribution of chemical enhancement factor (CHEF) to the overall SSEF is small even for organothiols on noble metal nanoparticles [14]. However, in the present experiments, it is the ratio between CHEF on both surfaces (GC and GC/AuNPs) contributes into the overall SSEF and we believe this will be an insignificant number.

In order to estimate SSEF, we will develop a monolayer of 4α-Co^{II}TAPc, an electro- and Raman- active molecule, on a GC and GC/AuNPs surfaces. To have RRS effect, a 785 nm laser line is employed for excitation since it matches well with the Q band of 4α-Co^{II}TAPc molecule [11]. Here plasmon inactive GC surface will demonstrate RRS alone whereas plasmon active GC/AuNPs will demonstrate both RRS and SERS i.e., SERRS. Further, cyclic voltammetry experiments are carried out on both GC and GC/AuNPs substrates/electrodes. By integrating the charge under the redox wave of the electroactive chromophore 4α-Co^{II}TAPc, the surface coverage i.e., c_{RRS} and c_{SERRS} are accurately estimated. Now, equation 3 can be rearranged as:

$$\text{SSEF} = \frac{I_{SERRS} \cdot \Gamma_{RRS}}{I_{RRS} \cdot \Gamma_{SERRS}} \qquad (4)$$

Where, Γ_{RRS} and Γ_{SERRS} are the surface coverage of probe molecule on GC and GC/AuNPs surfaces, respectively.

2. Experimental Section

1,8,15,22-Tetraaminophthalocyanatocobalt(II) (4α-Co^{II}TAPc), was synthesized according to the reported procedure [15, 16]. The diamond polished glassy carbon (GC) discs having a geometric of diameter 0.785 cm^2 was used as common surface/electrode for both Raman and electrochemical studies. All electrochemical experiments were carried out in a μAutolab potentiostat (Metrohm Autolab) with a custom-made three-electrode cell setup. All Raman measurements were performed using the Renishaw InVia Raman system equipped with 785 nm and 514 nm laser lines as excitation sources. SERS substrate was prepared by potentiostatic (-80 mV) deposition of gold nanoparticles over GC (GC/AuNPs) in 0.1 M HClO$_4$ containing 4 mM HAuCl$_4$ for 400 s. The self-assembled monomolecular film (SAM) of 4α-Co^{II}TAPc was formed

by soaking the cleaned GC and GC/AuNPs substrates in 1 mM DMF solution of 4α-Co^{II}TAPc overnight. In order to reduce the error in quantification of SSEF, the same substrates were used for RRS/SERRS and cyclic voltammetry experiments. In addition, RRS/SERRS experiments were performed first then followed by cyclic voltammetry so that the effect of electrochemical reaction on the orientation of the molecule, and hence the Raman signal, is excluded.

3. Results and Discussion

3.1. Estimation of real surface area of the SERS substrates

The surface morphology of GC/AuNPs substrate was characterized by scanning electron microscopy (SEM) experiments (Fig. 1). The SEM picture clearly reveals a defect-free uniform deposition of Au nanostructures in the size ranging from 10 to 100 nm.
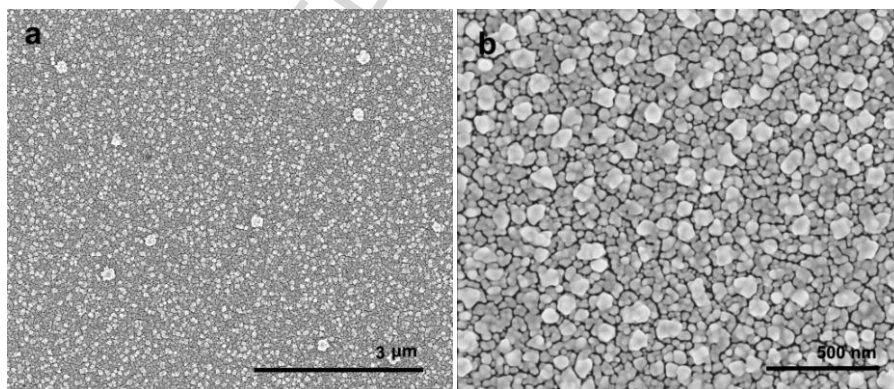
Fig. 1. SEM images of nanostructured Au electrodeposited over mirror polished GC.

It is well established in the literature [17, 18] that real surface area of gold can be achieved electrochemically by integrating the charge under the gold oxide reduction peak. In the present study, a similar electrochemical approach has been followed to quantify the real surface area of GC/AuNPs substrate [17, 18]. We used diamond polished GC surfaces in all our experiments since they have very smooth surface with negligible surface roughness. Therefore,

in the case of diamond polished GC, the geometric area and real surface area are almost similar. However, it is important to note that the real surface of SERS-active substrate is not equivalent to its geometric surface since SERS-active substrate is always highly roughened. In most of the earlier SSEF calculation methods, the difference between the real and geometric areas was not clearly accounted.

By integrating the charge under the gold oxide reduction peak, the real surface of Au in the GC/AuNPs substrate was found to be 3.02 cm^2 which is 3.98 times higher than its known geometric surface area of 0.785 cm^2 [18]. As diamond polished GC is known for its highly polished surface, the surface roughness is almost negligible in the case of GC surface.

3.2. Estimation of surface coverage of 4α-Co^{II}TAPc on both GC and GC/AuNPs surfaces

The ability of 4α-Co^{II}TAPc to form monomolecular film on GC and GC/AuNPs surfaces, via chemisorptions, and subsequent precise quantification of its surface coverage by cyclic voltammetry is well documented in the literature [11-13]. Since the real surface area of both the surfaces (GC and GC/AuNPs) has now been identified, the surface coverage of the 4α-Co^{II}TAPc monomolecular film on GC (Γ_{RRS}) and GC/AuNPs (Γ_{SERRS}) surfaces can also be quantified by integrating the charge under redox waves of the obtained cyclic voltammogram in Fig. 2A. The cyclic voltammograms (CVs) of GC/4α-Co^{II}TAPc and GC/AuNPs/4α-Co^{II}TAPc electrodes were performed in 0.1 H_2SO_4 (Fig. 2A). The CVs showed a pair of well-defined redox couple with an $E_{1/2}$ value around 0.34 V corresponding to Co^{III}/Co^{II} redox couple [13, 15]. The surface coverage (Γ) of 4α-Co^{II}TAPc SAM on GC and on GC/AuNPs electrodes has been estimated by integrating the charge under the anodic wave (Co^{II} oxidation) of the cyclic voltammogram. The Γ values of 2.25×10^{-10} mol cm^{-2} and 8.61×10^{-11} mol cm^{-2} have been estimated for 4α-Co^{II}TAPc SAM on

8

GC and on GC/AuNPs surfaces/electrodes, respectively. The values are in good agreement with the reported values [13]. The increased surface coverage on glassy carbon electrode is attributed in part to the additional π-stacking effect of 4α-Co^{II}TAPc on glassy carbon surface [13]. Conversely, the contribution of π-stacking on gold surface is insignificant.
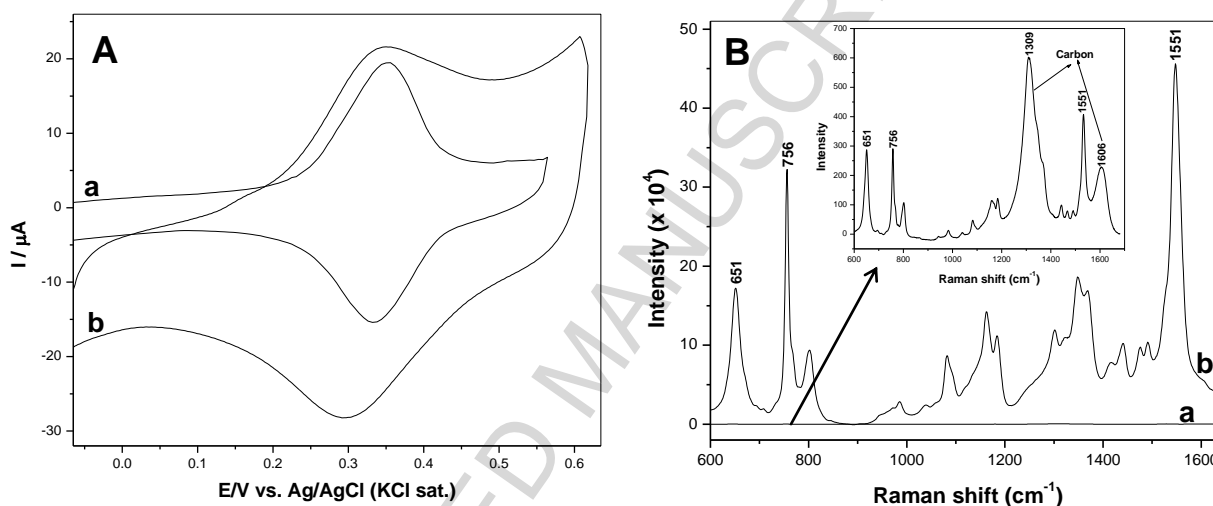

Fig. 2A. Cyclic voltammograms of 4α-Co^{II}TAPc SAM on (a) GC and (b) GC/AuNPs electrodes in 0.1 M H$_2$SO$_4$ at a scan rate of 0.1 Vs^{-1}. **B.** (a) RRS and (b) SERRS spectrum of 4α-Co^{II}TAPc SAM on GC and GC/AuNPs surfaces acquired using 785 nm laser line as excitation source. Inset shows the closer view of RRS spectrum.

3.3. Quantification of SERS substrate enhancement factor (SSEF)

Fig. 2B shows the RRS and SERRS spectra of 4α-Co^{II}TAPc SAM on GC and GC/AuNPs surfaces, respectively. Both RRS and SERRS spectra of 4α-Co^{II}TAPc on both surfaces showed two intense bands at 1551 cm^{-1} and 756 cm^{-1} corresponding to macrocycle in-plane stretching and macrocycle deformation, respectively [19-21]. Moreover, in the the RRS spectrum of 4α-Co^{II}TAPc on GC surface, the macrocycle in-plane stretching band at is 1551 cm^{-1} positioned in between the two intense bands at 1309 cm^{-1} and 1606 cm^{-1} corresponding to the stretching and

9

breathing modes of sp^2 hybridized carbon [22]. Thus, 1551 cm^{-1} band intensity may have some influence from sp^2 hybridized carbon vibrational bands on GC surface and the measurement of 1551 cm^{-1} band intensity may not be very accurate from time to time. On the other hand, the macrocycle deformation band at 756 cm^{-1} is intense and also has no interference from the underlying carbon surface. Therefore, to quantify the SSEF, the band at 756 cm^{-1} is used as a reference.

Now all the parameters in the equation 4 are known and have been estimated experimentally. By employing equation 4, SSEF of GC/AuNPs surface has been calculated and it was found to be $(2.82 \pm 0.22)10^4$. It is worth to mention at this juncture that all the 50 SERRS spectra recorded at different spots on the GC/AuNPs surface have similar intensity ratio among the different stretching bands confirming that all the 4α-Co^{II}TAPc molecules adopt same orientation over the entire substrate. We have also carried out the Raman experiment of 4α-Co^{II}TAPc SAM on GC surface at non-resonance condition using 514 nm laser line as the excitation source. The absence of Raman bands corresponding to the 4α-Co^{II}TAPc molecule, even after increasing the laser accumulation to 10 times higher than that used for the RRS measurement with 785 nm laser line, confirms that there is no charge-transfer enhancement on GC surface. This clearly implies that only resonance Raman effect contribute to the Raman spectrum of 4α-Co^{II}TAPc SAM on GC surface under red light excitation (785 nm). Further, it is worth to mention here that the overall estimated SSEF by the present method is the average value from whole surface and not at a particular spot. Therefore, the quantified SSEF by the present method is the average SSEF (ASSEF).

5. Conclusions

In summary, we have derived a most simplified equation, of improved precision, for the quantification of SSEF by a renewed approach. This approach uses electroactive and SERRS active 4α-Co^{II}TAPc as a probe molecule. The number of 4α-Co^{II}TAPc molecules involved in RRS and SERRS have been precisely quantified by electrochemical experiments. Our approach relies on performing RRS on plasmon inactive conductive surface and subsequently deducting RRS from SERRS to end up with surface enhancement. The present approach for SSEF quantification can be extended to the quantification of SSEF from various conducting and non-conducting SERS substrates at various excitation wavelengths, provided that a redox-active and resonance Raman active molecule is need for each laser line.

Acknowledgments

References

[1] S.-C. Luo, K. Sivashanmugan, J.-D. Liao, C.-K. Yao, H.-C. Peng, Nanofabricated SERS-active substrates for single-molecule to virus detection in vitro: A review, Biosensors and Bioelectronics, 61 (2014) 232-240.

[2] A. Sivanesan, E. Witkowska, W. Adamkiewicz, Ł. Dziewit, A. Kamińska, J. Waluk, Nanostructured silver-gold bimetallic SERS substrates for selective identification of bacteria in human blood, Analyst, 139 (2014) 1037-1043.

[3] W.B. Cai, B. Ren, X.Q. Li, C.X. She, F.M. Liu, X.W. Cai, Z.Q. Tian, Investigation of surface-enhanced Raman scattering from platinum electrodes using a confocal Raman microscope: dependence of surface roughening pretreatment, Surface Science, 406 (1998) 9-22.

[4] A.D. McFarland, M.A. Young, J.A. Dieringer, R.P. Van Duyne, Wavelength-Scanned Surface-Enhanced Raman Excitation Spectroscopy, The Journal of Physical Chemistry B, 109 (2005) 11279-11285.

[5] E.C. Le Ru, P.G. Etchegoin, Quantifying SERS enhancements, MRS Bulletin, 38 (2013) 631-640.

[6] E.C. Le Ru, E. Blackie, M. Meyer, P.G. Etchegoin, Surface Enhanced Raman Scattering Enhancement Factors: A Comprehensive Study, The Journal of Physical Chemistry C, 111 (2007) 13794-13803.

[7] P. Hildebrandt, M. Stockburger, Surface-enhanced resonance Raman spectroscopy of Rhodamine 6G adsorbed on colloidal silver, The Journal of Physical Chemistry, 88 (1984) 5935-5944.

[8] A. Sivanesan, H.K. Ly, J. Kozuch, M. Sezer, U. Kuhlmann, A. Fischer, I.M. Weidinger, Functionalized Ag nanoparticles with tunable optical properties for selective protein analysis, Chemical Communications, 47 (2011) 3553-3555.

[9] G. Kalaivani, A. Sivanesan, A. Kannan, N.S. Venkata Narayanan, A. Kaminska, R. Sevvel, Plasmon-tuned silver colloids for SERRS analysis of methemoglobin with preserved nativity, Langmuir, 28 (2012) 14357-14363.

[10] A. Sivanesan, J. Kozuch, H.K. Ly, G. Kalaivani, A. Fischer, I.M. Weidinger, Tailored silica coated Ag nanoparticles for non-invasive surface enhanced Raman spectroscopy of biomolecular targets, RSC Advances, 2 (2012) 805-808.

[11] A. Sivanesan, S. Abraham John, Amino group position dependent orientation of self-assembled monomolecular films of tetraaminophthalocyanatocobalt(II) on Au surfaces, Langmuir, 24 (2008) 2186-2190.

[12] A. Sivanesan, S. Abraham John, Electrochemical and spectral studies of self-assembled monolayer of 1,8,15,22-tetraaminophthalocyanatocobalt(II) on indium tin oxide surface, Journal of Electroanalytical Chemistry, 634 (2009) 64-67.

[13] A. Sivanesan, S.A. John, Adsorption thermodynamics and kinetics study for the self-assembly of 1,8,15,22-tetraaminophthalocyanatocobalt(II) on glassy carbon surface, Electrochimica Acta, 54 (2009) 7458-7463.

[14] F.S. Ameer, W. Hu, S.M. Ansar, K. Siriwardana, W.E. Collier, S. Zou, D. Zhang, Robust and Reproducible Quantification of SERS Enhancement Factors Using a Combination of Time-Resolved Raman Spectroscopy and Solvent Internal Reference Method, The Journal of Physical Chemistry C, 117 (2013) 3483-3488.

[15] A. Sivanesan, S. Abraham John, Amino group positions dependent morphology and coverage of electropolymerized metallophthalocyanine (M = Ni and Co) films on electrode surfaces, Electrochimica Acta, 53 (2008) 6629-6635.

[16] A. Sivanesan, S.A. John, Determination of l-dopa using electropolymerized 3,3',3",3"'-tetraaminophthalocyanatonickel(II) film on glassy carbon electrode, Biosensors and Bioelectronics, 23 (2007) 708-713.

[17] S. Trasatti, O.A. Petrii, Real surface area measurements in electrochemistry, Journal of Electroanalytical Chemistry, 327 (1992) 353-376.

[18] J.C. Hoogvliet, M. Dijksma, B. Kamp, W.P. Van Bennekom, Electrochemical pretreatment of polycrystalline gold electrodes to produce a reproducible surface roughness for self-assembly: A study in phosphate buffer pH 7.4, Analytical Chemistry, 72 (2000) 2016-2021.

[19] C. Jennings, R. Aroca, A.-M. Hor, R.O. Loutfy, Raman spectra of solid films 3—Mg, Cu and Zn phthalocyanine complexes, Journal of Raman Spectroscopy, 15 (1984) 34-37.

[20] M.P. Somashekarappa, S. Sampath, Orientation dependent electrocatalysis using self-assembled molecular films, Chemical Communications, 0 (2002) 1262-1263.

[21] X. Li, W. Xu, X. Wang, H. Jia, B. Zhao, B. Li, Y. Ozaki, Ultraviolet-visible and surface-enhanced Raman scattering spectroscopy studies on self-assembled films of ruthenium phthalocyanine on organic monolayer-modified silver substrates, Thin Solid Films, 457 (2004) 372-380.

[22] D.R. Tallant, J.E. Parmeter, M.P. Siegal, R.L. Simpson, The thermal stability of diamond-like carbon, Diamond and Related Materials, 4 (1995) 191-199.

<u>Highlights</u>

- AuNPs were potentiostatically deposited on GC surface

- 4α-Co^{II}TAPc SAM was formed on GC and GC/AuNPs

- RRS and SERRS studies were carried out on GC and GC/AuNPs surfaces, respectively

- Real surface area of GC/AuNPs and surface coverage of 4α-Co^{II}TAPc were electrochemically determined

- SERS enhancement factor was quantified by deducing RRS from SERRS